Chapter 1 Introduction

1.1 Development and Application of III-Nitride Semiconductor

The devices based on Silicon and GaAs operate only in the red and near-infrared spectral regions and cannot tolerate elevated temperatures or chemically hostile environments due to their low bandgap, uncontrolled generation of intrinsic carriers, and low resistance to caustic chemicals. Among the wide band gap semiconductor, the III-V nitrides have long been viewed as a very promising semiconductor system for device applications in the blue and UV wavelengths. The Nitride-base wide band gap semiconductor whose direct band gaps range from 1.9 eV (InN) to 6.2 eV (AlN). Thus, the III-V nitrides could potentially be fabricated into optical devices that are operating at wavelengths ranging from the red all the way into the UV and in electronic devices capable of operation at high temperatures, at high power levels, and in harsh environments [1-10]. It including full color semiconductor displays; lasers for reading or storing data on high density optical media; signal/automotive lighting, by combing the output of red, yellow, and blue LEDs; solar blind detectors; biological monitoring; and high temperature/high power electronics.

For bright blue light-emitting diodes (LEDs) based on III-nitrides used in place of incandescent light bulbs and paved the way for full-color displays as well as for the mixing of the three primary colors to obtain white light for illumination by semiconductor LEDs. These LEDs would provide compactness and longer lifetimes ＞10000 hours compared with 2000 hours for incandescent light bulbs. It also

consume only 15-20% of the power for the same luminous flux, resulting in significant energy saving. Short-wavelength laser diodes (LDs) based on III-nitrides are essential for high density optical storage applications because the diffraction-limited optical storage density increases quadratically as the probe laser wavelength is reduced [11-12].

The key breakthrough in making these devices can be attributed to the advent of nitride growth techniques. In particular, metalorganic vapor phase epitaxy (MOVPE) has been proved to be capable of growing excellent GaN, InGaN and AlGaN materials for fabrication of nitride-based devices.

1.2 Status of Study on III-Nitrides

The large differences in lattice parameters (~14%) and in thermal expansion coefficients (~36%) between GaN and sapphire forecast serious difficulties in the growth of high-quality films for optoelectronic applications (see Table 1). When GaN is directly deposited on the Al_2O_3 substrates, the growth isn't a two dimensional epilayer and the device performance using the grown films is poor. The lattice-mismatched problems have been greatly resolved by the introduction of AlN as an intermediate layer by Yoshida *et al*. in 1983 [13].

In 1989, Amano and Akasaki [14] introduced low-temperature AlN nucleation layer to produce the first smooth film and allowed control of impurity incorporation during growth. Further improvements were achieved with the introduction of

low-temperature GaN buffer layers by Nakamura [15] in 1991. The corresponding carrier concentration and electron mobility in this case were 4×10^{16} cm^{-3} and ~ 600 $cm^2/V\cdot s$, respectively. Such advances made GaN adequate for device application. The so-called two-step growth method was since widely employed to grow the heteroepitaxial GaN on sapphire substrate. However, it was found that the film quality dependents strongly on the nucleation conditions such as thickness [15,16], deposited temperature [17,18], and subsequent thermal treatment processes [19,20]. Besides the nucleation layer effects, the growth temperature is found to have a remarkable influence on the crystal structure [21,22]. High quality GaN film can be obtained only at growth temperature above 1,000℃ with a window of less 100℃ [23,24]. Other growth parameters such as the V/III source gas ratio [25,26] and the growth rate [27] as well as the mixing of N_2 and H_2 carrier gas [26,28], can also bring dramatic effect in affecting the film performance and crystalline properties.

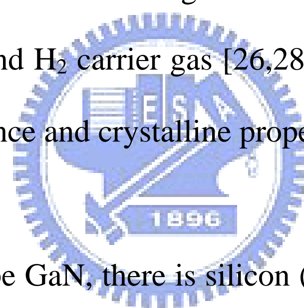

Among the potential n-type GaN, there is silicon (Si) and germanium (Ge), which are well known to give excellent results for the n-type doping of other classical III-V materials. Although they should be able to act as etiher donors or acceptors depending upon which atom they substitute (Ga or N), they mainly replace the gallium, due to the low covalent radii difference between Si and Ga (0.15 Å) or Ge and Ga (0.04 Å), compared with the radii difference with nitrogen. Murakami *et al* [29]. studied the incorporation of Si into GaN, and noticed the occurrence of cracks and pits at high Si concentrations. Nakamura *et al* [30]. used SiH_4 to dope GaN layers grown on GaN buffer layers and observed neither cracks nor pits even at high concentration (carrier concentration up to 2×10^{19} cm^{-3}). From their studies, the incorporation efficiency of Si is extremely high (10 times higher than that of Ge). Moreover, the PL is dominated by deep levels at 550 nm (the so-called ’yellow luminescence’) in both cases. The

overall luminescence intensity also increases with the doping level.

When MOCVD is employed a post growth treatment is necessary in order to convert the high resistance as-grown GaN:Mg to lower resistance *p*-type GaN (~1 Ω-cm). The high resistivity and low hole concentration in *p*-GaN are ascribed that hydrogen neutralizes the Mg acceptor [31,32]. This acceptor neutralization by H is similar to that in silicon [33]. To activate the acceptors, H must be removed by the post-growth treatments, either using a low energy electron beam irradiation (LEBBI) [34,35] or thermal annealing (TA) in an N_2 ambience at temperatures typically between 700 and 900℃ [31]. Rapid thermal annealing (RTA) [36] and minority carrier injection [37,38] methods can also be used to electrically activate the Mg dopants. These post-growth treatments cause dissociation of the Mg-H complexes [31,32] formed during MOVPE growth due to the use of ammonia (NH_3) source precursor [31,39]. When MBE is used, as-grown GaN exhibits *p*-type behavior presumably due to the absence of H in the hydrogen-free growth environment [40]. Nevertheless, Neugebauer and Van de Walle pointed out that H is beneficial for *p*-type doping by Mg when compared to the H-free case, since the Mg concentration increases and nitrogen vacancy concentration decreases in the presence of hydrogen [41,42]. Although it has been mentioned frequently that Mg and H form a complex in GaN:Mg films, the mechanisms of complex formation and release of H upon post-growth treatment have not been definitively cleared yet.

In the past few years, the PL interpretation of GaN:Mg has been controversial. People showed some relationship between the resistivity and the 450 nm peak in the PL spectra [43]. Amano *et al* [44]. also showed a PL peak around 390 nm when the Mg concentration was lower than 2×10^{16} cm^{-3} , while the peak was around 420-430

nm for Mg concentration of 7 $\times$ 10^{19} cm^{-3} . Although the optical binding energy of the Mg acceptor is about 250 meV, the activation energy from Hall data is 150~180 meV at the high doping levels (> 10^{19} cm^{-3}) [45]. The discrepancy between the thermal ionization energy and the optical ionization energy may be accounted for by the lattice relaxation associated with doping impurities in GaN. Pankove suggested that the strong potential fluctuation is present in highly Mg doped GaN, because of considerable electrical disorder [46]. This fluctuation indicates that the highly Mg doped GaN is compensated. If the Mg acceptor level is believed to be approximately 150 meV above the valence band, why the conduction band to acceptor level transition would be at 420-430 nm or longer. It is possible that the peak around 430 nm is from the transitions between the conduction band to impurity related defect level transition. This implies the presence of a Mg related defect level approximately 500 meV above the valence band. At this time, the nature of the Mg related defect level is still unknown, but some of the possibilities include a defect composed of more than one Mg atom, a Mg substituting for N as opposed to substituting for Ga, or Mg sitting on an interstitial site. These are discussed in the X-ray absorption spectra by Pan *et al* [47,48]. There may be no definite relationship between the 430 nm PL peak and the corresponding hole concentration. GaN:Mg has been studied using time-resolved PL [49] whose results yield an optical ionization energy of about 290 meV for the Mg acceptor level and approximately 550 meV for the Mg related defect complex. Kaufmann *et al.* assigned the 2.8 eV peak to deep-donor-acceptor pair recombination when Mg concentration was higher than 1 $\times$ 10^{19} cm^{-3}. As a result, the deep donor (430 meV) is attributed to a nearest-neighbor associate of a Mg_{Ga} with a V_N [50]. People also studied the deep level defects in Mg-doped GaN by photocapacitance and deep level transient spectroscopy (DLTS) [51,52].

Recently, the persistent photoconductivity (PPC) behavior was also ob-served in GaN:Mg and interpreted as the metastability [53,54]. The PPC observed in undoped GaN was attributed to metastable behavior associated with a capture barrier of ~ 0.2 eV [55,56]. This could be a severe problem for the hole activation. From the theoretical predictions, Park *et al* [57]. claimed that the on-site position of substitutional acceptors should be stable. Moreover, continuous blueshift with the increasing excitation power density has been observed [50], and explained in terms of the formation of mini-bands [58].

Isoelectronic doping technique has been used on many conventional III-V compound semiconductors for reducing defect density [59-65]. For instance, the background concentration and deep trap concentration in GaN can be effectively reduced by adding the isoelectronic impurity [66,67]. The isoelectronic impurities can be the anion atoms (e.g. InP:Bi) or cation atoms (e.g. ZnSe:Mg). The common interpretation of isoelectronic doping processes is based on the electronegativity and lattice distortion [68-70]. An isoelectronic center can form bound states because of a short range central-cell potential. The primary factors affecting the binding potential are the electronegativity and the size difference between the impurity and the host ion which it replaces. From the experimental data, the isoelectronic impurity potential is attractive to a hole (electron) if its electronegativity is small (larger) than that of the host atom. It is also found that only large different size atoms produce isoelectronic traps since the large lattice distortion is formed by substitution. After an isoelectronic trap has captured an electron or a hole, the trap becomes negative or positive. It then will capture a carrier of opposite charge forming a bound exciton or the trapped electron (hole) will recombine radiatively with a hole (an electron) located at a distant acceptor (donor) forming D-iso-trap pair or iso-trap-A pair. Jadwisienczak *et al.*

discussed the isoelectronic As, P, and Bi replacing N in GaN using a simple spherical potential-well model. Their estimation of the isoelectronic trap binding energy is very close to the experimental data.

After our firrst investigation of isoelectronic In doping effects in GaN [66], people began to study the related topics. Widmann *et al*. examined the surfactant e¤ect of In during the GaN growth by rf-MBE [71]. Shen *et al*. also reported the promising improvement on the optical and electrical properties after In incorporation [72]. Kumano *et al*. found that the spontaneous emission lifetime increased and the threshold excitation density reduced in In-doped GaN [73]. Pozina *et al*. found that the influence of In is stronger for GaN grown in N-rich conditions [74]. So the isoelectronic In doping is indeed helpful for GaN growth not only by MOVPE but also by MBE system.

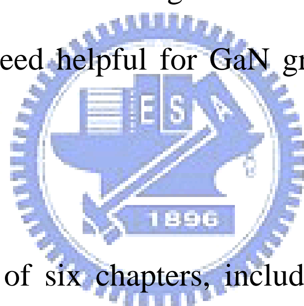

This dissertation consists of six chapters, including the present one. Chapter 2 introduces several common epitaxy techniques and basic MOVPE-growth processes such as reaction pathways, possible growth mechanism, and growth rate. In Chapter 3, we give detailed description for our experiments including our sample preparations, and the characterization equipments, such as the scanning electron microscopy (SEM), X-ray diffraction, photoluminescence (PL), Raman scattering, and Hall measurement. The epitaxial growth of Si modulation doping GaN samples are described in chapter 4, where the growth parameter effects such as growth temperature and V/III source gas ratio, optical property, electronic property and their structure transition. Chapter 5 discusses the MOVPE-grown GaN:Mg and In isoelectronic doping GaN:Mg. The both GaN:Mg and In doped GaN:Mg films were characterized by mean of secondary ion mass spectroscopy (SIMS), scanning electron microscopy (SEM), Raman, and PL

measurements. The annealing behaviors and other Mg(+In)-doping effects such as local microstructure change, Mg-induced defects, and In doping effects were investigated by Hall measurement. The excitation power dependence of the Mg related emission and the intensity reduction behavior of Mg(+In)-doped GaN of various Mg(In) concentration are also discussed. Several model simulations for examining the possible Mg occupation cases were also presented in this chapter. In the final chapter, we conclude our investigations on the nitride materials.

References

1. H. Morkoc, S. Strite, G. B. Gao, M. E. Lin, B. Sverdlov, and M. Burns, *J. Appl. Phys.* **76**, 1363 (1994).
2. T. Matsuoka, *J. Cryst. Growth* **124**, 433 (1992).
3. I. Akasaki and H. Amano, *J. Cryst. Growth* **146**, 455 (1995).
4. Y. Kuga, T. Shirai, M. Haruyama, H. Kawanishi and Y. Suematsu, *Jpn. J. Appl. Phys.* **34**, 4085 (1995).
5. A. Bykhovski, B. Gelmont, and M. Shur, *Appl. Phys. Lett.* **63**, 2243 (1993).
6. M. A. Khan, A. Bhattaral, J. N. Kuznia, and D. T. Olson, *Appl. Phys. Lett.* **63**, 1214 (1993).
7. J. C. Zolper, R. J. Shul, A. G. Baca, R. G. Wilson, S. J. Pearton, and R. A. Stall, *Appl. Phys. Lett.* **68**, 2273 (1996).
8. S. Yoshida and J. Suzuki, *J. Appl. Phys.* **84**, 2940 (1998).
9. S. Nakamura, M. Senoh, S. I. Nagahama, T. Matsushita, K. Kiyoku, Y. Sugimoto, T. Kozaki, H. Umemoto, M. Sano, and T. Mukai, *Jpn. J. Appl. Phys.* **38**, L1966 (1999).
10. S. Strite, M. E. Lin and M. Morkoc, *Thin Solid Films* **231**, 197 (1993).
11. S. Nakamura, M. Senoh, S. I. Nagahama, N. Iwasa, T. Yamada, T. Matsushita, Y. Sugimoto and H. Kiyoku, *Appl. Phys. Lett.* **70**, 866 (1997).
12. S. Nakamura, M. Senoh, S. I. Nagahama, N. Iwasa, T. Yamada, T. Matsushita, H. Kiyoku, Y. Sugimoto, T. Tozaki, H. Umemoto, M. Sano and K. Chocho, *Jpn. J. Appl. Phys.* **37**, L627 (1998).
13. S Yoshida, S. Misawa, and S. Gonda, *Appl. Phys. Lett.* **42**, 427 (1983).
14. H. Amano, M. Kito, K. Hiramatsu, and I. Akasaki, *Jpn. J. Appl. Phys.* **28**, L2112 (1989).
15. S. Nakamura, *Jpn. J. Appl. Phys.* **30**, L1705 (1991).
16. H. Amano, N. Sawaki, and I. Akasaki, *Appl. Phys. Lett.* **48**, 353 (1986).
17. B. P. Keller, S. Keller, D. Kapolnek, W. -N. Jlang, Y. -F. Wu, H. Masui, X. Wu, B. Heying, J. S. Speck, U. K. Misjra, and S. P. DenBaars, *J. Electron. Mater.* **24**, 1707 (1995).
18. D. K. Gaskill, A. E. Wickenden, K. Doverspike, B. Tadayon, and L. B. Rowland, *J. Electron. Mater.* **24**, 1525 (1995).
19. A. E. Wickenden, D. K. Wickenden, and T. J. Kistenmacher, *J. Appl. Phys.* **75**, 5367 (1994).
20. C. F. Lin, G. C. Chi, M. S. Feng, J. D. Guo, J. S. Tsang, and J. M. Hong, *Appl. Phys. Lett.* **68**, 3758 (1996).
21. H. C. Lin, J. Ou, W. K. Chen, W. H. Chen, and M. C. Lee, *Jpn. J. Appl. Phys.* **36**,

L598 (1997).

22. C. H. Hong, K. Wang, and D. Pavlidis, *J. Electron. Mater.* **24**, 213 (1995).
23. A. Dissanayake, J. Y. Lin, and H. X. Jiang, *Appl. Phys. Lett.* **65** , 2317 (1994).
24. Z. J. Yu, B. S. Sywe, A. U. Ahmed, and J. H. Edgar, *J. Electron. Mater.* **21**, 383 (1992).
25. O. Briot, J. P. Alexis, M. Tchounkeu, R. L. Aulombard, *Mater. Sci. & Eng. B* **43**, 147 (1997).
26. R. Niebuhr, K. Bachem, K. Dombrowski, M. Maier, W. Pletschen, and U. Kaufmann, *J. Electron. Mater.* **24**, 1531 (1995).
27. I. Berishev, E. Kim, and A. Bensaoula, *J. Vac. Sci. Technol. A* **16**, 2791 (1998).
28. T. Sasaki and S. Zembutsu, *J. Appl. Phys.* **61**, 2533 (1987).
29. H. Murakami, T. Asahi, H. Amano, K. Hiramaysu, N. Sawaki, and L. Akasaki, *J. Cryst. Growth.* **115,** 648 (1991).
30. S. Nakamura, T. Mukai, M. Senoh, and N. Iwasa, *Jpn. J. Appl. Phys.* **31,** 2883 (1992).
31. S. Nakamura, N. Iwasa, M. Senoh, and T. Mukai, *Jpn. J. Appl. Phys.* **31**, 1258 (1992).
32. M. S. Brandt, N. M. Johnson, R. J. Molnar, R. Singh, and T. D. Moustakas, *Appl. Phys. Lett.* **64**, 2264 (1994).
33. J. I. Pankove, P. J. Zanzucchi, and C. W. Magee, *Appl. Phys. Lett.* **46**, 421 (1985).
34. S. Nakamura, M. Senoh, and T. Mukai, *Jpn. J. Appl. Phys.* **30**, L1708 (1991).
35. H. Amano, M. Kito, K. Hiramatsu, and I. Akasaki, *Jpn. J. Appl. Phys.* **28**, L2112 (1989).
36. W. Götz, N. M. Johnson, J. Walker, D. P. Bour, and R. A. Street, *Appl. Phys. Lett.* **68**, 667 (1996).
37. S. J. Pearton, J. W. Lee, C. Yuan, *Appl. Phys. Lett.* **68**, 2690 (1996).
38. M. Miyachi, T. Tanaka, Y. Kimura, H. Ota, *Appl. Phys. Lett.* **72**, 1101 (1998).
39. W. Götz, N. M. Johnson, J. Walker, D. P. Bour, H. Amano, and I. Akasaki, *Appl. Phys. Lett.* **67**, 2666 (1995).
40. M. A. L. Johnson, J. D. Brown, N. A. El-Masry, J. W. Cook, Jr., J. F. Schetzina, H. S. Kong, and J. A. Edmond, *J. Vac. Sci. Technol. B* **16**, 1282 (1998).
41. J. Neugebauer and C. G. Van de Walle, *Phys. Rev. Lett.* **75**, 4452 (1995).
42. J. Neugebauer and C. G. Van de Walle, *Appl. Phys. Lett.* **68**, 1829 (1996).
43. S. Nakamura, N. Iwasa, M. Senoh, and T. Mukai, *Jpn. J. Appl. Phys.* **31**, 1258 (1992).
44. H. Amano, M. Kitoh, K. Hiramatsu, I. Akasaki, *J. Electrochem. Soc.* **137**, 1639 (1990).
45. M. Ilegems, R. Dingle, *J. Appl. Phys.* **44**, 4234 (1973).

46. J. I. Pankove, *Phys. Rev*. **140**, A2059 (1965).
47. Y. C. Pan, S. F. Wang, W. H. Lee, M. C. Lee, W. K. Chen, W. H. Chen, L. Y. Jang, J.F. Lee, C. I. Chiang, H. Change, K. T. Wu, and D. S. Lin, *Appl. Phys. Lett*. **78,** 31 (2001).
48. Y. C. Pan, S. F. Wang, W. H. Lee, W. C. Lin, C. I. Chiang, H. Chang, H. H. Hsieh, J. M. Chen, D. S. Lin, M. C. Lee, W. K. Chen, and W. H. Chen. *Solid Stat. Commun.* (2001).
49. M. Smith, G. D. Chen, J. Y. Lin, H. X. Jiang, A. Salvador, B. N. Sverdlov, A. Botchkarev, H. Morkoc, and B. Goldenberg, *Appl. Phys. Lett.* **68**, 1883 (1996).
50. U. Kaufmann, M. Kunzer, M. Maier, H. Obloh, A. Ramakrishnan, B. Santic, and P. Schlotter, *Appl. Phys. Lett.* **72**, 1326 (1998).
51. G.-C. Yi and B. W. Wessels, *Appl. Phys. Lett*. **68**, 3769 (1996).
52. W. G.. otz, N. M. Johnson, and D. P. Bour, *Appl. Phys. Lett.* **68**, 3470 (1996).
53. C. Johnson, J. Y. Lin, H. X. Jiang, M. Asif Khan, C. J. Sun, *Appl. Phys. Lett.* **68**, 1808 (1996).
54. J. Z. Li, J. Y. Lin, H. X. Jiang, A. Salvador, A. Botchkarev, H. Morkoc, *Appl. Phys. Lett.* **69**, 1474 (1996).
55. G. Beadie, W. S. Rabinovich, A. E. Wickenden, D. D. Koleske, S. C. Binari, and J. A.Freitas, Jr., *Appl. Phys. Lett.* **71**, 1092 (1997).
56. M. T. Hirsch, J. A. Wolk, W. Walukiewicz, and E. E. Haller, *Appl. Phys. Lett.* **71**, 1098 (1997).
57. C. H. Park, D. J. Chadi, *Phys. Rev. B* **55**, 12995 (1997).
58. E. Oh, H. Park, and Y. Park, *Appl. Phys. Lett*. **72**, 70 (1998).
59. D. G. Thomas, J. J. Hopfield, and C. J. Frosch, *Phys. Rev. Lett*. **15**, 857 (1965).
60. D. R. Scifres, . Holonyak, Jr. C. B. Duke, G. Kleiman, A. B. Kunz, M. G. Graford, W. O. Groves, and A. H. Herzog, *Phys. Rev. Lett*. **27**, 191 (1971).
61. M. K. Lee, T. H. Chiu, A. Dayem, and E. Agyekum, *Appl. Phys. Lett*. **53**, 2653 (1988).
62. W. Walukiewicz, *Appl. Phys. Lett*. **54**, 2009 (1989).
63. P. K. Bhattacharya, S. Dhar, P. Berger, and F.-Y. Juang, *Appl. Phys. Lett*. **49**, 470 (1986).
64. W. Liu, N. Chen, *J. Cryst. Growth.* **154,** 19 (1995).
65. H. Ehrenreich, amd J. P. Hirth, *Appl. Phys. Lett*. **46**, 668 (1985).
66. C. K. Shu, J. Ou, H. C. Lin, W. K. Chen, and M. C. Lee, *Appl. Phys. Lett.* **73**, 641 (1998).
67. H. Kumano, K.-I. Koshi, S. Tanaka, I. Suemune, X.-Q. Shen, P. Riblet, P. Ramvall, and Y. Aoyagi, *Appl. Phys. Lett*. **75**, 2879 (1999).
68. H. Beneking, P. Narozny and N. Emeis, *Appl. Phys. Lett.* **47**, 828 (1985).

69. W. M. Jadwisienczak and H. J. Lozykowski, *Mat. Res. Soc. Symp. Proc*. **482**, 1033 (1998).
70. T. Ogino and M. Aoki, *Jpn. J. Appl. Phys*. **18**, 1049 (1979).
71. F. Widmann, B. Daudin, G. Feuillet, N. Pelekanos, and J. L. Rouviere, *Appl. Phys. Lett.* **73**, 2642 (1998).
72. X. Q. Shen, P. Ramvall, P. Riblet, and Y. Aoyagi, *Jpn. J. Appl. Phys*. **38**, L411 (1999).
73. H. Kumano, K.-I. Koshi, S. Tanaka, I. Suemune, X.-Q. Shen, P. Riblet, P. Ramvall, and Y. Aoyagi, *Appl. Phys. Lett.* **75**, 2879 (1999).
74. G. Pozina, J. P. Bergman, B. Monemar, S. Yamaguchi, H. Amano, and I. Akasaki, *Appl. Phys. Lett.* **76**, 3388 (2000).

Substrate Material	Symmetry	Lattice Parameters(Å)	Coefficient of Thermal expansion
Wurtzite InN	Hexagonal	a=3.53 c=5.69	3.7×10^{-6} /K 5.7×10^{-6} /K
Wurtzite GaN	Hexagonal	a=3.189 c=5.185	5.59×10^{-6} /K 3.17×10^{-6} /K
Wurtzite AlN	Hexagonal	a=3.112 c=4.982	4.2×10^{-6} /K 5.3×10^{-6} /K
α-Al_2O_3	Hexagonal	a=4.758 c=12.99	7.3×10^{-6} /K 8.1×10^{-6} /K
6H-SiC	Hexagonal	a=3.080 c=15.12	4.2×10^{-6} /K 4.68×10^{-6} /K
ZnO	Hexagonal	a=3.252 c=5.213	2.90×10^{-6} /K 4.75×10^{-6} /K
Si	Cubic	a=5.430	3.59×10^{-6} /K
GaAs	Cubic	a=5.563	6.0×10^{-6} /K
3C-SiC	Cubic	a=34.36	~2.4×10^{-6} /K
InP	Cubic	a=5.869	4.50×10^{-6} /K
GaP	Cubic	a=5.451	4.65×10^{-6} /K
MgO	Cubic	a=4.622	10.5×10^{-6} /K
$MgAl_2O_4$	Cubic	a=8.083	7.45×10^{-6} /K

Table 1 Properties of prospective nitride substrates

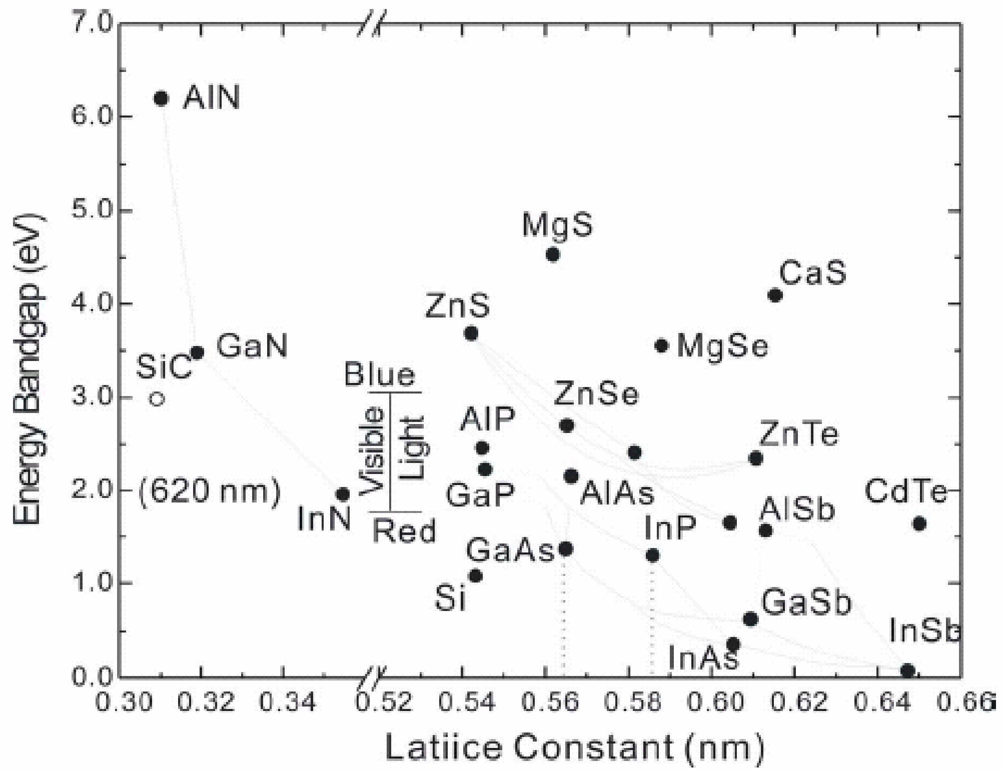

Fig 1 Energy band gap versus lattice constant for III-V semiconductor compounds and alloys.